# Finite Volume Solvers for the Shallow Water Equations Using Matrix Radial Basis Function Reconstruction

L. Bonaventura, E. Miglio and F. Saleri

MOX - Dipartimento di Matematica
Politecnico di Milano
P.zza Leonardo da Vinci 32
20133 Milano Italy
luca.bonaventura@polimi.it
edie.miglio@polimi.it
fausto.saleri@polimi.it

The accuracy of low order numerical methods for the shallow water equations is improved by using vector reconstruction techniques based on matrix valued radial basis functions. Applications to geophysical fluid dynamics problems show that these reconstruction techniques allow to maintain important discrete conservation properties while greatly reducing the error with respect to low order discretizations.

## 1 Finite volume methods for shallow water models

The shallow water equations result from the Navier-Stokes equations when the hydrostatic assumption holds and only barotropic and adiabatic motions are considered. They can be written as

$$\frac{\partial h}{\partial t} + \nabla \cdot \Big( H \mathbf{v} \Big) = 0, \tag{1}$$

$$\frac{\partial \mathbf{v}}{\partial t} + (\mathbf{v} \cdot \nabla)\mathbf{v} = -f\mathbf{k} \times \mathbf{v} - g\nabla h. \tag{2}$$

Here, $\mathbf{v}$ denotes the two-dimensional velocity vector, $\mathbf{k}$ is the radial unit vector perpendicular to the plane on which $\mathbf{v}$ is defined (or to the local tangent plane, in case of applications in spherical geometry), $h$ is the height of the fluid layer above a reference level, $H = h - h_s$ is the thickness of the fluid layer, $h_s$ is the orographic or bathymetric profile, $g$ is the gravitational constant and $f$ is the Coriolis parameter. Eulerian-Lagrangian discretizations for the shallow water equations using formulation (1), (2) have been proposed in [5],

[6], which couple a mass conservative, semi-implicit discretization on unstructured Delaunay meshes to an Eulerian-Lagrangian treatment of momentum advection. The resulting methods are highly efficient because of their mild stability restrictions, while mass conservation allows for their practical (and successful) application to a number of pollutant and sediment transport problems. A key step of the Eulerian-Lagrangian method is the interpolation at the foot of characteristic lines, which in the papers quoted above is performed by RT0 elements (see e.g. [9]) or by low order interpolation procedures based on area weighted averaging. These interpolators have at most first order convergence rate and can introduce large amounts of numerical diffusion, thus making their application questionable especially for long term simulations. Another widely used formulation for applications to large scale atmospheric dynamics is the so called *vector invariant form* (see e.g. [11]), in which the momentum equation is rewritten as:

$$\frac{\partial \mathbf{v}}{\partial t} = -(\zeta + f)\mathbf{k} \times \mathbf{v} - \nabla\Big(gh + K\Big). \tag{3}$$

Here, $\zeta$ is the component of relative vorticity in the direction of $\mathbf{k}$ and $K$ denotes the kinetic energy. This formulation is usually the starting point for the derivation of energy, potential enstrophy and potential vorticity preserving discretizations (see e.g. [1]). Eulerian discretizations of equations (1),(3) have been proposed in [3, 4], which preserve discrete approximations of mass, vorticity and potential enstrophy. These properties are important for numerical models of general atmospheric circulation, especially for applications to climate modelling. The two time level, semi-implicit scheme proposed in these papers used RT reconstruction to compute the nonlinear terms in the discretization of (3).

In this paper, vector interpolators based on the technique of matrix valued Radial Basis Functions (RBF) proposed in [7] are applied to improve the accuracy of the above mentioned Eulerian or Eulerian-Lagrangian finite volume solvers. The use of matrix RBF interpolators allows to achieve this goal without having to resort e.g. to higher order RT elements, which would make more difficult or impossible to preserve the important discrete conservation properties of the methods reviewed above. For simplicity, in this paper we restrict ourselves to the two dimensional case, although all the results and the methods can be generalized to 3D. Although in general this is not sufficient to raise the convergence order of the overall methods, models employing RBF reconstructions display significantly smaller errors and have in general less numerical dissipation, making their use attractive for a number of applications. More extensive tests of the accuracy of matrix valued RBF reconstructions have been reported in [2].

## 2 Matrix valued Radial Basis Functions for vector field reconstruction

In this section, the vector reconstruction based on RBF proposed in [7] is briefly summarized in a context that is appropriate for the applications to hydrodynamic models. Similar applications of scalar RBF reconstructions have been presented e.g. in [10].

Consider a set of $N$ distinct points in the plane $x_i, i = 1, \ldots, N,\ \ x_i \in \mathbf{R}^2$, and assume that for each $x_i$ a two dimensional unit vector $\mathbf{n}_i$ is given. Consider then a smooth vector field $\mathbf{u} : \mathbf{R}^2 \to \mathbf{R}^2$. The interpolation data are the values $u_i = \mathbf{u}(x_i) \cdot \mathbf{n}_i$. The interpolation problem consists of the reconstruction of the field $\mathbf{u}(x)$ at an arbitrary point $x \in \mathbf{R}^2$, given the values $u_i$. This problem can be reformulated as follows: consider the vector valued distribution denoted formally by $\boldsymbol{\lambda}_i = \delta(x - x_i) \cdot \mathbf{n}_i$, whose action on a vector valued function $\mathbf{f}(x)$ is such that $(\boldsymbol{\lambda}_i, \mathbf{f}) = \mathbf{f}(x_i) \cdot \mathbf{n}_i$. Given a matrix valued radial basis function

$$\boldsymbol{\Phi}(x) = \begin{bmatrix} \phi_{11}(x)\ \phi_{12}(x) \\ \phi_{21}(x)\ \phi_{22}(x) \end{bmatrix},$$

where the functions $\phi_{ij}$ are e.g. Gaussian or multiquadric kernels, the convolution $\boldsymbol{\Phi} * \boldsymbol{\lambda}_i$ is defined according to [7] as

$$\boldsymbol{\Phi} * \boldsymbol{\lambda}_i(x) = \begin{bmatrix} \phi_{11}(x - x_i)n_i^1 + \phi_{12}(x - x_i)n_i^2 \\ \phi_{21}(x - x_i)n_i^1 + \phi_{22}(x - x_i)n_i^2 \end{bmatrix}$$

where $\mathbf{n}_i = [n_i^1, n_i^2]^T$. The interpolation problem consists then of finding coefficients $c_j, j = 1, \ldots, N$ and a vector valued polynomial $\mathbf{p}(x)$ such that the vector valued distribution denoted formally by $\boldsymbol{\lambda} = \sum_{j=1}^{N} c_j \boldsymbol{\lambda}_j$ and the polynomyal $\mathbf{p}$ satisfy the conditions $(\boldsymbol{\lambda}_i, \boldsymbol{\Phi} * \boldsymbol{\lambda} + \mathbf{p}) = u_i, \quad i = 1, \ldots, N$. Furthermore, if $\mathbf{u}$ is actually a polynomial, the polynomial $\mathbf{p}$ determined by this procedure should coincide with $\mathbf{u}$. These conditions can be rewritten as

$$\sum_{j=1}^{N} c_j (\boldsymbol{\lambda}_i, \boldsymbol{\Phi} * \boldsymbol{\lambda}_j + \mathbf{p}) = u_i, \quad i = 1, \ldots, N.$$

It can be seen that determination of the coefficients $c_j, j = 1, \ldots, N$ requires the inversion of the interpolation matrix $\mathbf{A} = (a_{i,j})_{i,j=1,\ldots,N}$ whose entries are given by $a_{i,j} = (\boldsymbol{\lambda}_i, \boldsymbol{\Phi} * \boldsymbol{\lambda}_j)$. Conditions under which this matrix is symmetric and positive definite are given in [7]. In the simple case in which it is assumed that no polynomial constraint is imposed and that $\boldsymbol{\Phi} = \phi \mathbf{I}$, where $\mathbf{I}$ is the identity matrix and $\phi$ is a single scalar radial basis function, the problem reduces for example to $\sum_{j=1}^{N} c_j \phi(x_i - x_j)\mathbf{n}_i \cdot \mathbf{n}_j = u_i, \quad i = 1, \ldots, N$.

## 3 Applications to environmental modelling

Numerical results obtained with the models described in section 1 will now be presented. In all cases, it will be shown that RBF vector reconstruction leads to a substantial improvement of the accuracy of the considered methods. For all the tests, we employed a reconstruction using the Gaussian or multiquadric RBF. The polynomial reproduction constraint, when applied, imposed exact reproduction of constant vectors. A simple 9 point stencil has been adopted, using the normal velocity components to the edges of the triangle on which the reconstruction is being carried out and to the edges of its nearest neighbours (i.e. of the triangles which have common edges with it).

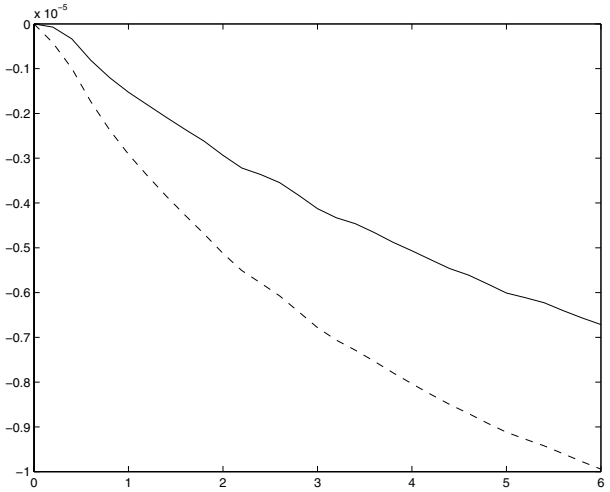


**Fig. 1.** Relative decay in total energy for Eulerian-Lagrangian model, computed using RT reconstruction (full line) and RBF reconstruction with 9 points stencil (dotted line) in a free oscillations test.

Firstly, the results obtained with the Eulerian-Lagrangian method of [6] will be discussed. In this context, the RBF reconstruction can be used as opposed to RT0 elements when performing the interpolation at the foot of the characteristics. In a first test, a square domain of width 20 m was considered, which was discretized by an unstructured triangular mesh with 3984 elements and 2073 nodes. A constant basin depth of 2 m was assumed. At the initial time, still water was assumed and the free surface profile was taken to be a gaussian hill centered at the center of the domain, with amplitude 0.1 m and standard deviation 2 m. In absence of any explicit dissipative term, the total energy of the system should be conserved. The free oscillations of the fluid were simulated for a total of 6 s with a time step $\Delta t = 0.01$ s. The time evolution of total energy is shown in figure 1, while the height field computed

at various timesteps is shown in figures 2, 3. It can be observed that the energy dissipation caused by the interpolation of the Eulerian-Lagrangian method is reduced by 40% if the RBF reconstruction is used, while the values of the maxima and minima in the height field are improved by approximately 20%.

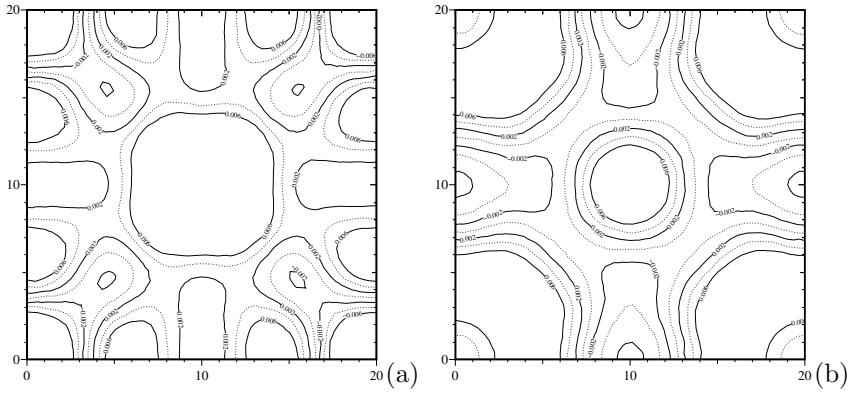


**Fig. 2.** Height field computed using RT reconstruction for the Eulerian-Lagrangian method in free oscillations test at time (a) $t = 4$ s and (b) $t = 6$ s.

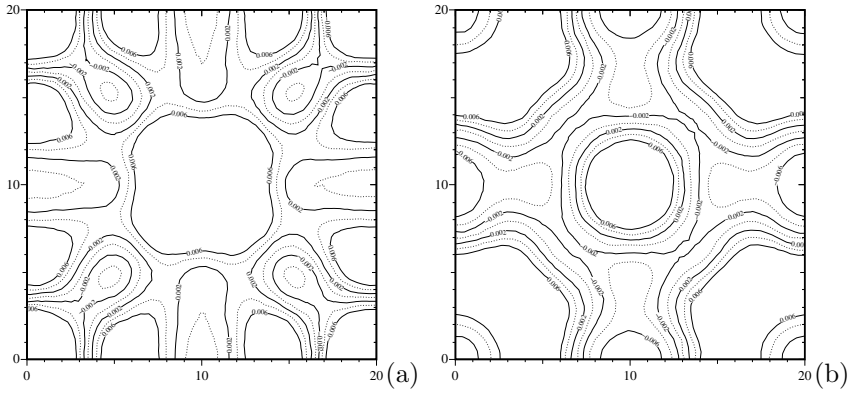


**Fig. 3.** Height field computed using RBF reconstruction with 9 points stencil for Eulerian-Lagrangian method in a free oscillations test at time (a) $t = 4$ s and (b) $t = 6$ s.

Similar experiments have also been carried out with an Eulerian discretization of the shallow water equations in spherical geometry. In this particular case, a three-time level, semi-implicit time discretization was coupled to the potential enstrophy preserving spatial discretization of [4], using either the Raviart Thomas algorithm or a vector RBF reconstruction of the velocity

field necessary for the solution of equation (3). The algorithm performance was studied when applied to test case 3 of the standard shallow water suite [11], which consists of a steady-state, zonal geostrophic flow with a narrow jet at midlatitudes. For this test case, an analytic solution is available, so that errors can be computed by applying the numerical method at different resolutions (denoted by the refinement level in a dyadic refinement procedure starting from the regular icosahedron, see [4] for a complete description of the grid construction). The values of the relative error in various norms as computed at day 2 with different spatial resolutions and with time step $\Delta t = 1800$ s is displayed in Tables 1, 2 for Raviart Thomas algorithm and vector RBF reconstruction, respectively. It can be observed that, although the convergence rates remain approximately unchanged (due to the fact that the approximately second order discretization of the geopotential gradient was the same in both tests), the errors both in the height and velocity fields have decreased by an amount that ranges between 30% and 50% approximately.

**Table 1.** Relative errors in shallow water test case 3 with RT reconstruction for nonlinear terms.

| Level | $l_2$ error, $h$ | $l_2$ error, $\mathbf{v}$ | $l_\infty$ error, $h$ | $l_\infty$ error, $\mathbf{v}$ |
|---|---|---|---|---|
| 3 | 7.42e-3 | 0.25 | 2.53e-2 | 0.33 |
| 4 | 1.94e-3 | 5.9e-2 | 8.1e-3 | 9.1e-2 |
| 5 | 6.05e-4 | 1.27e-2 | 2.9e-3 | 1.87e-2 |
| 6 | 2.54e-4 | 3.19e-3 | 1.24e-3 | 4.17e-3 |

**Table 2.** Relative errors in shallow water test case 3 with 9 points RBF reconstruction for nonlinear terms.

| Level | $l_2$ error, $h$ | $l_2$ error, $\mathbf{v}$ | $l_\infty$ error, $h$ | $l_\infty$ error, $\mathbf{v}$ |
|---|---|---|---|---|
| 3 | 7.27e-3 | 0.16 | 2.08e-2 | 0.17 |
| 4 | 1.52e-3 | 3.38e-2 | 6.74e-3 | 5.77e-2 |
| 5 | 4.05e-4 | 7.7e-3 | 1.7e-3 | 1.22e-2 |
| 6 | 1.45e-4 | 2.11e-3 | 4.8e-4 | 2.89e-3 |

We have then considered the nonstationary test case 6 of [11], for which the inital datum consists of a Rossby - Haurwitz wave of wavenumber 4. This type of wave is an analytic solution for the barotropic vorticity equation and can also be used to test shallow water models on a time scale of up to 10-15 days. Plots of the meridional velocity component at simulation day 5 are

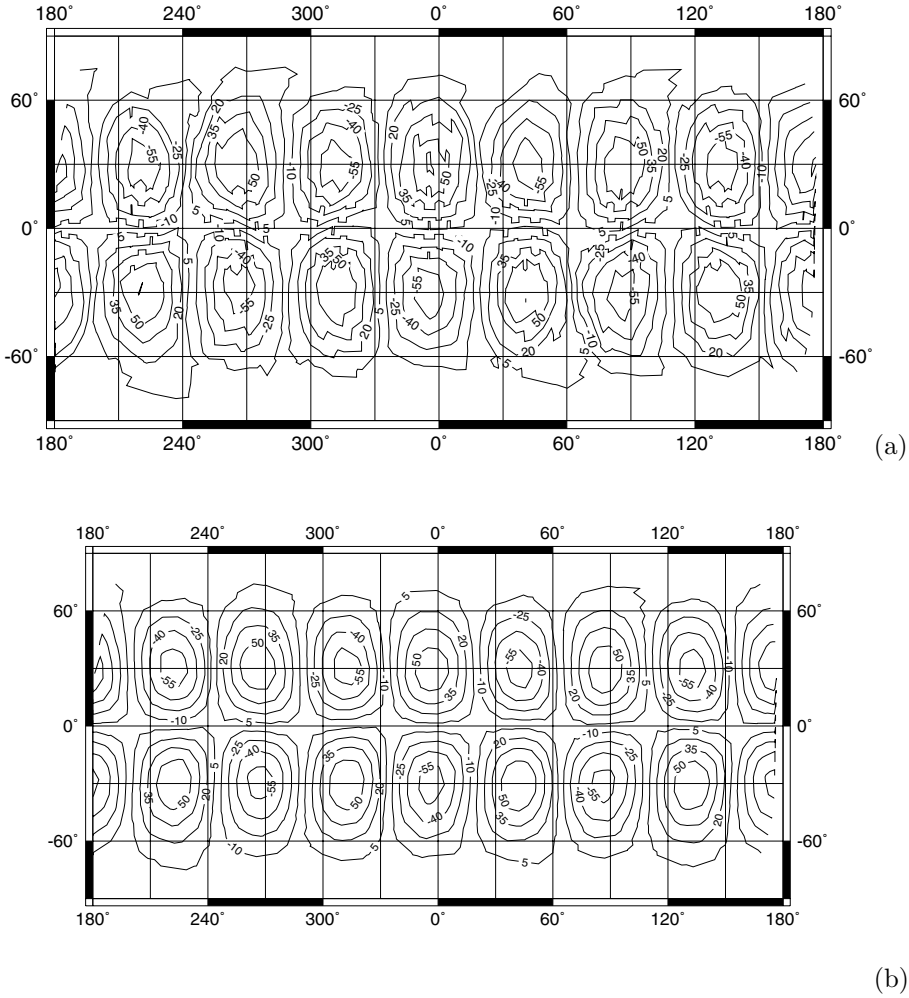


**Fig. 4.** Meridional velocity in shallow water test case 5, computed using (a) RT0 reconstruction (b) RBF reconstruction with 9 points stencil. Contour lines spacing is 15 m $s^{-1}$.

shown in figure 4, as computed with a timestep of $\Delta t = 600$ s on a spherical quasi-uniform triangular mesh with a spatial resolution of approximately 400 km. It can be observed for example that, when using RT0 reconstruction, the meridional velocity field obtained is much less regular than in the case of matrix RBF reconstruction, which compares better with results obtained in reference high resolution simulations. Furthermore, the total energy loss is reduced in the RBF computation by approximately 30%, thus improving the energy conservation properties of the model, which conserves potential enstrophy but not energy as discussed in [4].

Concerning the computational cost of RBF reconstructions, it should be observed that, in the case of Eulerian models, it is possible to carry out most of the RBF computations at startup, so that the extra computational cost due to the use of RBFs is approximately 20% of the cost of a model run using simple RT0 reconstruction. On the other hand, in the case of Eulerian-Lagrangian models, the extra computational cost is higher than in the Eulerian case, since the RBF coefficients have to be recomputed at each time step for each of the trajectory departure points.

## References

1. Arakawa, A., Lamb, V.: A potential enstrophy and energy conserving scheme for the shallow water equations. Monthly Weather Review, **109**, 18–136 (1981)
2. Baudisch, J.: Reconstruction of Vector Fields Using Radial Basis Functions. MA Thesis, Munich University of Technology, Munich (2005)
3. Bonaventura, L., Kornblueh, L., Heinze, T., Ripodas, P.: A semi-implicit method conserving mass and potential vorticity for the shallow water equations on the sphere, Int. J. Num. Methods in Fluids, **47**, 863–869 (2005)
4. Bonaventura, L., Ringler, T.: Analysis of discrete shallow water models on geodesic Delaunay grids with C-type staggering, Monthly Weather Review, **133**, 2351–2373 (2005)
5. Casulli, V., Walters, R.A.: An unstructured grid, three-dimensional model based on the shallow water equations, Int. J. Num. Methods in Fluids, **32**, 331–348 (2000)
6. Miglio, E., Quarteroni, A., Saleri, F.: Finite element approximation of quasi-3d shallow water equations, Comp. Methods in Appl. Mech. and Eng., **174**, 355–369 (1999)
7. Narcowich, F.J., Ward, J.D.: Generalized Hermite interpolation via matrix-valued conditionally positive definite functions, Math. Comp., **63**, 661–687 (1994)
8. Pedlosky, J.: Geophysical Fluid Dynamics. Springer Verlag, New York - Berlin (1987)
9. Quarteroni, A., Valli, A.: Numerical approximation of partial differential equations. Springer Verlag, New York - Berlin (1994)
10. Rosatti, G., Bonaventura, L., Cesari, D.: Semi-implicit, semi-Lagrangian environmental modelling on cartesian grids with cut cells, J. Comp. Phys., **204**, 353–377 (2005)
11. Williamson, D.L., Drake, J.B., Hack, J.J., Jakob, R., Swarztrauber, P.N.: A Standard Test Set for Numerical Approximations to the Shallow Water Equations in Spherical Geometry, J. Comp. Phys., **102**, 211–224 (1992)